Structural and vibrational properties of single walled nanotubes under hydrostatic pressure

S. Reich*, C. Thomsen* and P. Ordejón†

*Institut für Festkörperphysik, Technische Universität Berlin, 10623 Berlin, Germany
†Institut de Ciència de Materials de Barcelona (CSIC), Campus de la U.A.B. E-08193 Bellaterra, Barcelona, Spain

Abstract. We studied the high-energy Raman modes of single walled carbon nanotubes by pressure experiments and *ab initio* calculations. The uniform shift of all three Raman peaks under pressure is in contrast with what one might expect in strongly uniaxial systems. We show that this apparent discrepancy is resolved by the eigenvectors of chiral nanotubes, which are of mixed axial and circumferential character.

Raman scattering is widely used in the study of physical phenomena of carbon nanotubes as well as in sample characterization. For the latter, in particular, the frequency of the radial breathing mode is used to determine the tubes diameters.[1] The Raman spectrum above $1000\,\mathrm{cm}^{-1}$, in contrast, is rather insensitive to the growth methods and sample treatment. It shows a disorder mode around $1350\,\mathrm{cm}^{-1}$[2] and a series of peaks around $1600\,\mathrm{cm}^{-1}$, the high-energy modes. Their shape in this spectral range depends on the nanotubes being metallic or not. Despite the overall robustness of the Raman spectra and their frequent appearance in the literature, the exact origin of the high-energy vibrations is still not understood. The eigenvectors of these modes at the Γ point of the nanotubes may be derived from the graphene optical modes by introducing the confinement (or folding) around the tube's circumference. Inspite of a number of studies on the symmetry of the Raman scattered light the peculiar shape of the spectra remains an open question.[3]

In this paper we present a study of carbon nanotubes under high hydrostatic pressure combined with *ab initio* calculations of the high-energy phonon eigenvectors. The purpose of the presentation is two-fold: First we demonstrate how high-pressure experiments help our general understanding of Raman scattering by the high-energy vibrations; second we show the importance of chiral tubes in explaining experiments.

Three and six out of the 8 and 15 Raman active modes fall into the high-energy range in achiral and chiral nanotubes, respectively.[4] Representative Raman spectra at (almost) ambient pressure and two high-pressure points are displayed in Fig. 1a. Details on the experiments can be found in Ref. [5]; for an overview over other pressure experiments see Ref. [6]. Fig. 1b shows the frequency change of the high-energy modes under pressure in more detail; we - as others - find that the normalized pressure slope is the same for the three high-energy Raman peaks. As was pointed out by us recently, this seemingly ordinary result is in fact surprising for a highly anisotropic material like carbon nanotubes.[7] In uniaxial systems the different elastic properties along the

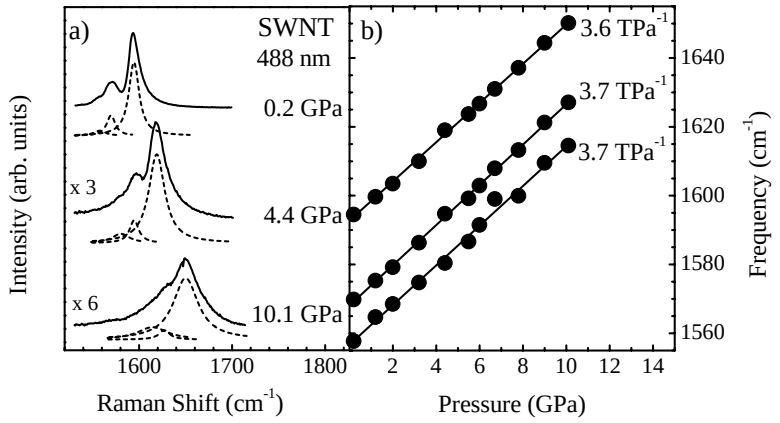

FIGURE 1. a) High-energy Raman modes in semiconducting nanotubes under hydrostatic pressures between 0.2 and 10 GPa (T=300 K). b.) Dependence of the Raman frequencies on pressure. The normalized pressure slopes of the three Raman peaks are the same within experimental error.

principal axis and perpendicular to it are, in general, manifested in different phonon frequency shifts under pressure.

To obtain a more quantitative picture of the expected pressure slopes we analyzed in Ref. [7] the strain which is introduced in a single walled nanotube by applying hydrostatic stress. All results, those of an elastic continuum model,[8] a calculation of the elastic constants,[9] and a molecular dynamics simulation,[10] agree in that the strain in the radial or circumferential direction $\varepsilon_{\theta\theta}$ of the nanotube is predicted to be ≈ 3 times larger than the axial strain ε_{zz}. We also performed *ab initio* calculations on small diameter ($d \approx 8$ Å) achiral and chiral nanotubes and found excellent agreement with the elastic continuum model when the smaller radii are taken into account.[11] Raman experiments on multiwalled tubes, where the pressure slopes of the high-energy modes are 25 % smaller than in single walled tubes, further verify the predicted strain tensors; the differences in the two types of tubes are nicely explained by the different geometries, namely, the much larger inner and outer radii of the multiwalled tubes.[8]

In Fig. 2 we depict a (6,6) and an (8,4) tube where the strain in the radial direction is two times larger than the axial strain. The applied hydrostatic pressure changes not

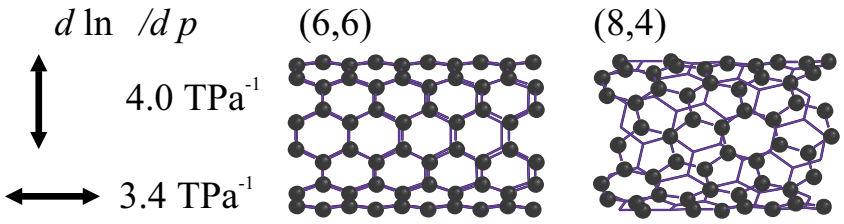

FIGURE 2. Schematic picture of the distortion of a (6,6) and an (8,4) tube under hydrostatic pressure, i.e., $\varepsilon_{\theta\theta} = 2\varepsilon_{zz}$. Note that the strain is fully symmetric in the point groups of the tubes, but not for the graphene hexagon. On the left we list the logarithmic pressure derivatives expected for modes where the atomic displacements is along the circumference of the tube (↕) and along the tube's axis (⟷).

only the area of the graphene hexagons, but also distorts their shape and lifts the six fold symmetry of the graphene unit cell. Such a shear strain splits the doubly degenerate E_{2g} graphene modes and allows us to estimate the pressure dependence of the high-energy nanotubes modes by zone-folding arguments.[7, 12]

Let us begin by considering armchair or zig-zag tubes. Here the atomic displacements for the phonon eigenvectors are always along the nanotube axis or perpendicular to it, because of the non-trivial stabilizer (mirror plane) of the carbon sites.[4, 13] This directly yields an expected pressure dependence for the modes vibrating in the circumferential, higher-strain direction which is $\approx 0.6\,\mathrm{TPa}^{-1}$ larger than for axial modes (compare Fig. 2). This result depends only on the direction of the atomic displacement with respect to the strain direction[1] and is independent of the chirality of the tubes. In other words, high-energy vibrations in single walled nanotubes which are either parallel or perpendicular to the nanotube axis must have different pressure slopes regardless of the tube chirality. This is obviously not the case in semiconducting nanotubes as shown above in Fig. 1b.[7] In order to explain the absence of the splitting in the pressure experiments a closer look at the phonon eigenvectors in chiral nanotubes is necessary: Chiral nanotubes – in contrast to the achiral nanotubes discussed so far – possess no mirror symmetry operations; they belong to the D_q point groups.[4] Moreover, the stabilizer of the carbon atoms in chiral tubes is only the trivial identity operation. Therefore, the direction of the atomic displacement is not restricted by symmetry. A distribution of atomic displacement directions averages out the splitting introduced by the shear strain. Only the average, hydrostatic component is then observable in a Raman experiment.[14] To prove or discard this explanation we calculated the phonon modes in chiral nanotubes by first-principal methods.

Ab initio calculations were performed for (8,4) and (9,3) chiral nanotubes with the SIESTA code as described in detail elsewhere.[15, 13] Compared to previous phonon calculations for nanotubes with this code we improved the basis set (double-ζ, polarized) and the real space cutoff (240 Ry).[16] We first calculated the phonon eigenvectors of a (6,6) and a (10,0) tube and found very good agreement (deviations $< 5\,\%$) with the symmetry imposed eigenmodes in achiral tubes.

In Fig. 3 we present two examples of the high-energy phonon eigenvectors in chiral nanotubes. On the left we show a non-degenerate A_1 eigenvector for a (9,3) tube. The atomic displacements indicated by the ticks at the atoms point neither along the *z* axis nor along the circumference. Instead the displacement direction coincides with the direction of the carbon-carbon bonds; the angle between the circumference and the displacement direction is $\alpha = 16^\circ$. In the (8,4) nanotube we found the corresponding modes, i.e., the tangential A_1 eigenvectors where the two graphene sublattices move out of phase, to be along the circumference ($\alpha = -3^\circ$) and the *z* axis (87°), respectively. The phonon eigenvectors in chiral nanotubes may thus not be divided into axial and circumferential or LO and TO-like vibrations. Instead, they are, in general, of mixed character.

We now turn to the degenerate modes in chiral nanotubes. As an example one of the E_1 high-energy eigenvectors of an (8,4) tube is shown in Fig. 3. Going from left to right

---

[1] This follows because graphene has only two linearly independent phonon deformation potentials: the Grüneisen parameter γ and one shear-strain potential.

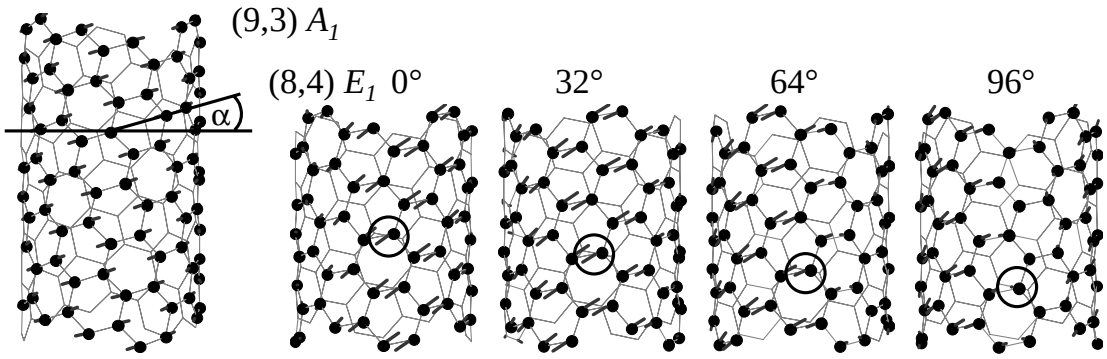

FIGURE 3. Left: A_1 mode of an (9,3) chiral nanotube (1627 cm^{-1}) with $\alpha = 16°$. The other four tubes show an E_1 eigenvector (1610 cm^{-1}) of the (8,4) tube. Going from left to right the tube was successively rotated by an angle of 32° around the z axis. As can be seen in the figure this angle corresponds to a helicical symmetry operation of the tube. The magnitude and the direction of the atomic displacements changes when going around the tube as can be seen by following the atoms marked by a circle.

we rotated the nanotube unit cell in steps of $\approx 32°$ around the z axis; the sequence of four pictures corresponds to going around the tube. In each picture we highlighted one atom to point out to the reader the circumferential or angular dependence of the atomic displacement. First, it can be seen that the magnitude of the displacement is changing as expected for an E_1 mode, which has two nodes around the circumference. But second, the direction of the displacement varies as well: In the first picture (0°) the displacement tick is almost perpendicular to one of the carbon-carbon bonds, whereas it is roughly parallel to a bond in the last two pictures of the sequence (64° and 94°).

The varying or "wobbling" of the displacement direction becomes more obvious when plotting the z component of the displacement versus the circumferential component (Fig. 4). In this plot a non-degenerate eigenmode corresponds to a single point, because both the magnitude and the direction of the displacement are constant within the unit cell [compare the (9,3) A_1 mode]. A degenerate but purely circumferential or axial

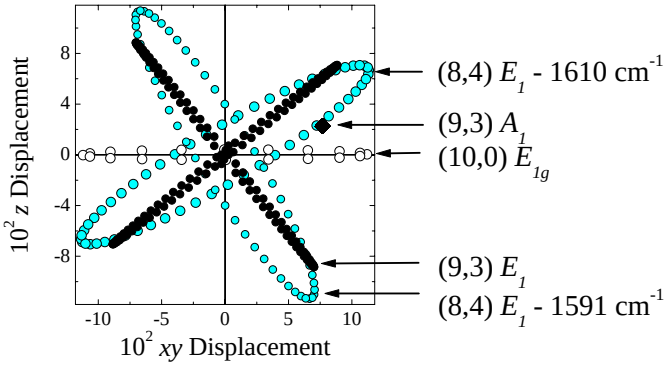

FIGURE 4. z versus the circumferential component of the displacement direction for six different phonon eigenmodes. A degenerate eigenvector is fully specified by its symmetry and the principal axes of the displacement ellipse.

eigenvector shows up as points on the x or y axis of the diagram; as an example we plotted the E_{1g} circumferential eigenvector of a (10,0) zig-zag tube. The large open ellipse labeled as the (8,4) E_1 with $\omega = 1610\,\mathrm{cm}^{-1}$ corresponds to the phonon eigenvector already shown in Fig. 3; its degenerate mode has the same ellipse. The ellipse of the second high-energy E_1 eigenmode ($1591\,\mathrm{cm}^{-1}$) is perpendicular to it. Finally, we plotted the E_1 modes of a (9,3) tube as an example of a degenerate mode with a large z and circumferential component, but a closed ellipse. Here the two components are in phase and the displacement direction is constant when going around the nanotube.

In conclusion we presented a study of the high-energy Raman modes in single walled carbon nanotubes. From the pressure dependence of the phonon frequencies it follows that the modes in chiral tubes are, in general, not of purely axial or circumferential character. We verified our considerations by *ab initio* phonon calculations of two chiral nanotubes. Indeed, the calculated eigenvectors were of mixed LO and TO character. For degenerate E modes we found that the direction of the atomic displacement may even "wobble" when going around the circumference. Finally, we introduced a method to specify an eigenvector by its symmetry and displacement ellipse.

We thank H. Jantoljak, I. Loa (MPI Stuttgart), and K. Syassen (MPI Stuttgart) for carrying out the pressure experiments. This work was supported by the MEC (Spain) and the DAAD (Germany) within the Acciones-Integradas Hispano-Alemanes. P. O. acknowledges support from Fundación Ramón Areces (Spain), EU project SATURN IST-1999-10593, and Spain-DGI project BFM2000-1312-002-01.

REFERENCES

1. M. Milnera, J. Kürti, M. Hulman, and H. Kuzmany, Phys. Rev. Lett. **84**, 1324 (2000).
2. C. Thomsen and S. Reich, Phys. Rev. Lett. **85**, 5214 (2000); C. Thomsen, S. Reich, and J. Maultzsch, in *Electronic Properties of Novel Materials-Progress in Molecular Nanostructures*, edited by H. Kuzmany, J. Fink, M. Mehring, and S. Roth, IWEPS Kirchberg, page xxxx, 2001.
3. G. S. Duesberg, I. Loa, M. Burghard, K. Syassen, and S. Roth, Phys. Rev. Lett. **85**, 5436 (2000); H. H. Gommans *et al.*, J. Appl. Phys. **88**, 2509 (2000); A. Jorio *et al.*, Phys. Rev. Lett. **85**, 2617 (2000); S. Reich, C. Thomsen, G. S. Duesberg, and S. Roth, Phys. Rev. B **63**, R041401 (2001).
4. M. Damnjanović, I. Milošević, T. Vuković, and R. Sredanović, Phys. Rev. B **60**, 2728 (1999).
5. C. Thomsen, S. Reich, A. R. Goñi, H. Jantoljak, P. Rafailov, I. Loa, K. Syassen, C. Journet, and P. Bernier, phys. stat. sol. (b) **215**, 435 (1999).
6. P. V. Teredesai *et al.*, phys. stat. sol. (b) **223**, 479 (2001); U. D. Venkateswaran *et al.*, phys. stat. sol. (b) **223**, 225 (2001).
7. S. Reich, H. Jantoljak, and C. Thomsen, Phys. Rev. B **61**, R13 389 (2000).
8. C. Thomsen, S. Reich, H. Jantoljak, I. Loa, K. Syassen, M. Burghard, G. S. Duesberg, and S. Roth, Appl. Phys. A **69**, 309 (1999).
9. J. Lu, Phys. Rev. Lett. **79**, 1297 (1997).
10. U. D. Venkateswaran, A. M. Rao, E. Richter, M. Menon, A. Rinzler, R. E. Smalley, and P. C. Eklund, Phys. Rev. B **59**, 10 928 (1999).
11. S. Reich, C. Thomsen, and P. Ordejón, unpublished.
12. F. Cerdeira, C. J. Buchenauer, F. H. Pollack, and M. Cardona, Phys. Rev. B **5**, 580 (1972).
13. S. Reich, C. Thomsen, and P. Ordejón, *Phonon eigenvectors of chiral nanotubes*, submitted.
14. E. Anastassakis, J. Appl. Phys. **81**, 3046 (1997).
15. D. Sánchez-Portal, P. Ordejón, E. Artacho, and J. Soler, Int. J. Quantum Chem. **65**, 453 (1999); E. Artacho, *et al.*, phys. stat. sol. (b) **215**, 809 (1999).
16. D. Sánchez-Portal, E. Artacho, J. M. Soler, A. Rubio, and P. Ordejón, Phys. Rev. B **59**, 12678 (1999).